NUMERICAL MODELLING OF FLUX EMERGENCE IN THE SOLAR ATMOSPHERE: EFFECTS OF PARTIAL IONISATION

James E. Leake

Space and Astrophysics, University of Warwick, Gibbet Hill Road, Coventry, CV4 7AL, England. Email: J.E.Leake@warwick.ac.uk

ABSTRACT

We present results from 2.5D numerical simulations of the emergence of magnetic flux from the upper convection zone through the photosphere and chromosphere into the corona. Certain regions of the solar atmosphere are at sufficiently low enough temperatures to be only partially ionised, in particular the lower chromosphere. This leads to Cowling resistivities 10^{12} orders of magnitude larger than the Coulomb values, and thus highly anisotropic diffusion of currents. We find that the rates of emergence of magnetic field are greatly increased by the partially ionised regions of the model atmosphere, and the resultant magnetic field is more diffuse. More importantly, the only currents associated with the magnetic field to emerge into the corona are aligned with the field, and thus the newly formed coronal field is force-free.

Key words: Sun, Plasmas, Magnetic fields, Sunspots.

1. INTRODUCTION

The evolution of the solar atmosphere, in particular the corona, is strongly influenced by the presence of magnetic field. This coronal field is believed to originate beneath the surface, where dynamo action at the base of the convection zone can generate large scale toroidal fields, as shown by Hughes and Proctor (1988) and Gilman, Morrow and Deluca (1989). The instabilities present in these fields give rise to the formation of magnetic flux tubes which are driven by buoyancy through the convection zone up to the surface and emerge in to the atmosphere above. This process is known as flux emergence. Flux emergence is widely regarded as the process by which new active regions on the Sun's surface are formed. The emerging fields evolve to form the complex structures we see in the Sun's atmosphere, such as coronal loops and prominences, and strongly influence dynamic events such as flares and coronal mass ejections.

Previous work has been performed under the MHD approximation. Under this assumption the atmosphere of the Sun is represented by a fully ionised plasma, consisting of electrons and ions only.

In this paper we relax the assumption of a fully ionised plasma. The lower chromosphere of the Sun's atmosphere is partially ionised, and depending on the local magnetic field can be weakly ionised (Khodachenko et al., 2004). This is not taken into account in the standard MHD model. The effect of the possible presence of neutrals in a plasma on the governing equations is investigated, and a new set of equations is derived to simulate flux emergence through the lower atmosphere of the Sun. As the presence of neutrals will affect momentum transfer due to relative velocities, we expect the emergence and evolution of magnetic field to be affected by these additions to the model. We present results on the rates of flux emergence and the nature of emerging flux tubes as they pass through the partially ionised region of the atmosphere and the resultant structure of the magnetic field.

2. NUMERICAL METHODS

2.1. Equations

The generalised Ohm's law for a fluid containing ions, electrons and neutral atoms is given by (Cowling, 1957)

$$\begin{aligned} \mathbf{E} + (\mathbf{v} \wedge \mathbf{B}) &= \eta \mathbf{j} + (\eta_c - \eta)\mathbf{j}_\perp \\ &= \eta \mathbf{j}_\parallel + \eta_c \mathbf{j}_\perp \end{aligned} \quad (1)$$

where $\mathbf{v}$ is the fluid velocity, $\mathbf{B}$ is the magnetic field,$\mathbf{E}$ is the electric field,$\mathbf{J} = (\nabla \wedge \mathbf{B})/\mu_0$ is the current density and

$$\mathbf{j}_\perp = \frac{\mathbf{B} \wedge \mathbf{j} \wedge \mathbf{B}}{|\mathbf{B}|^2} \quad (2)$$

is the component of the current density perpendicular to the magnetic field while

$$\mathbf{j}_\parallel = \frac{(\mathbf{j}.\mathbf{B})\mathbf{B}}{|\mathbf{B}|^2} \quad (3)$$

is the component parallel to the field.

Here η is the Coulomb resitivity

$$\eta = \frac{m_e(\nu'_{ei} + \nu'_{en})}{n_e e^2}. \quad (4)$$

η_c is the Cowling resistivity, defined by

$$\frac{{\xi_n}^2 {B_0}^2}{\alpha_n} = \eta_c - \eta. \quad (5)$$

where ξ_n is the fraction of neutrals.

$$\alpha_n = m_e n_e \nu'_{en} + m_i n_i \nu'_{in}. \quad (6)$$

and ν'_{ie}, ν'_{ie} and ν'_{ie} are the effective collisional frequencies defined by

$$\nu'_{kl} = \frac{m_l}{m_l + m_k} \nu_{kl} \quad (7)$$

where $k = e, i, l = i, n$. $m_{e,i,n}$ are masses of the electron, ions, and neutrals respectively.

This approach to Ohm's law gives an equation for the evolution of the magnetic field:

$$\begin{aligned} \frac{\partial \mathbf{B}}{\partial t} &= \nabla \wedge (\mathbf{v} \wedge \mathbf{B}) - \nabla \wedge (\eta \mathbf{j}_\parallel) \\ &- \nabla \wedge (\eta_c \mathbf{j}_\perp) \end{aligned} \quad (8)$$

Thus the Cowling resistivity η_c diffuses cross-field currents $\mathbf{j}_\perp$ and the Coulomb resistivity η diffuses field-aligned currents $\mathbf{j}_\parallel$. Using solar parameters taken from the VALC model of the Sun (Vernazza et al., 1981) and using a typical chromospheric magnetic field profile (Leake et al., 2005) η_c has the profile in Fig.1. At heights of 2000 km η_c/η can be as high as 10^{12} and in theses models η_c is less than numerical round-off. Hence in the following work the approximation $\eta = 0$ is used.

Adding the joule heating term for a partially ionised plasma (Braginskii, 1965)

$$\begin{aligned} Q &= (\mathbf{E} + (\mathbf{v} \wedge \mathbf{B})).\mathbf{j} \\ Q &= \eta {j_\parallel}^2 + \eta_c {j_\perp}^2 \end{aligned} \quad (9)$$

gives the set of equations for a partially ionised plasma:

$$\frac{\partial \rho}{\partial t} = -\nabla.(\rho \mathbf{v}) \quad (10)$$

$$\frac{\partial}{\partial t}(\rho \mathbf{v}) = -\nabla.(\rho \mathbf{v}\mathbf{v}) + (\mathbf{j} \wedge \mathbf{B}) \quad (11)$$

$$-\nabla P + \rho \mathbf{g} + \nabla.\mathbf{S} \quad (12)$$

$$\begin{aligned} \frac{\partial \mathbf{B}}{\partial t} &= \nabla \wedge (\mathbf{v} \wedge \mathbf{B}) - \nabla \wedge (\eta \mathbf{j}_\parallel) \\ &- \nabla \wedge (\eta_c \mathbf{j}_\perp) \end{aligned} \quad (13)$$

$$\begin{aligned} \frac{\partial}{\partial t}(\rho \epsilon) &= -\nabla.(\rho \epsilon \mathbf{v}) - P \nabla.\mathbf{v} \\ &+ \eta {j_\parallel}^2 + \eta_c {j_\perp}^2. \end{aligned} \quad (14)$$

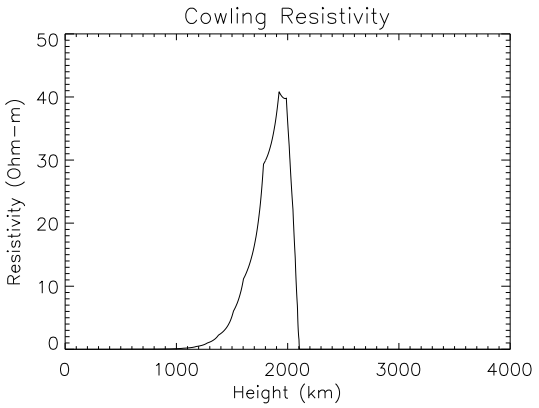

Figure 1. The Cowling conductivity as a function of height using the VALC model for density and temperature and a decreasing magnetic field strength.

where ρ is the gas density, ϵ is the specific internal energy density, which is proportional to the gas temperature, $\mathbf{g}$ is gravitational acceleration and $\mathbf{S}$ is the stress tenor. These are solved numerically using a Lagrangian-remap code (Arber et al., 2001).

In adddition, the effects of heating/cooling terms such as thermal conduction, radiative losses and small scale shock heating of acoustic modes etc. are modelled. This is done by relaxing the temperature to its initial value on a timescale τ which varies with height.

$$\frac{d\epsilon}{dt} = -\frac{\epsilon - \epsilon_0(\rho)}{\tau} \quad (15)$$

2.2. Initialisation

The eqns (10) to (14) are non-dimensionalised using values at the photosphere. $r_{ph} = 1.5 \times 10^5 m$, $t_{ph} = 23\,s$, $\rho_{ph} = 2.7 \times 10^{-4}\,kg/m^3$, $B_{ph} = 1200\,G$, $v_{ph} = 6514\,m/s$, $T_{ph} = 6420\,K$, $P_{ph} = 1.17 \times 10^4\,Pa$. Unless stated all values quoted are in dimensionless form, and multiplication by these values retains SI units.

The initial stratification is a simple 1D model of the temperature profile of the Sun, which includes the upper 3000 km of the convection zone, photosphere/chromosphere, transition zone, and corona. The temperature profile consists of a linear polytrope for the convection zone with a vertical gradient at the critical adiabatic value The temperature in the photosphere and chromosphere is assumed to be constant at a temperature of 1, as is the temperature in the corona at a temperature of 150. These two regions are connected by a transition region of width $w_{tr} = 5$. The density and gas pressure are specified by assuming hydrostatic equilibrium initially

$$\frac{dP}{dy} = -\rho g \quad (16)$$

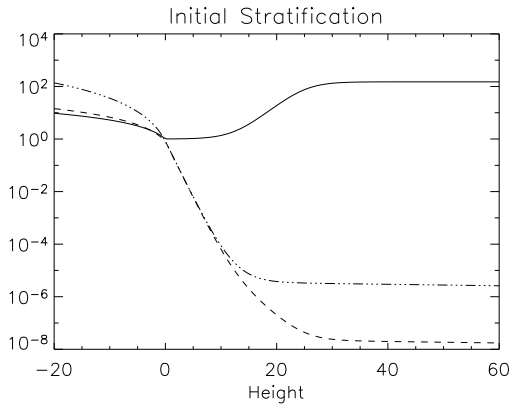

Figure 2. Distribution of temperature (solid line), density (dashed line) and gas pressure (triple-dot dashed line) all values are normalised.

and the ideal gas law

$$P = \rho T \tag{17}$$

which is given in normalised form. The vertical coordinate is y and x is the horizontal. Fig.2 shows the initial stratification in normalised units.

The evolution of a magnetic flux tube is initiated by inserting a uniformally twisted magnetic field profile in the convection zone, centred about $y = -12$.

$$B_z = B_0 \exp\left(-\frac{r^2}{a^2}\right) \tag{18}$$

$$B_\phi = qrB_r \tag{19}$$

where r is the radial distance from the centre of the tube, B_z is the magnetic field component in the axial direction (z), and B_ϕ is the azimuthal component. The width of the tube a is chosen to be 2, and the strength of the field at the centre of the tube, B_0, is 5. Following the approach of Archontis et al. (2004), the value of the twist, q, is chosen so that the tube is stable to drag in the convection zone which would otherwise fragment an untwisted tube (Moreno-Insertis and Emonet, 1996). In these simulations this corresponds to a value of $q = -1/a$ so the tube has a left hand twist.

The plasma pressure inside the tube differs from the field-free pressure by $p_1(r)$, where

$$\frac{dp_1(r)}{dr} = \mathbf{j} \wedge \mathbf{B}, \tag{20}$$

so that the pressure gradient matches the Lorentz force. The change in density inside the flux tube relative to the field free atmosphere is specified by assuming the tube to be in thermal equilibrium with its surroundings.

$$T_0(z) = \frac{p_0(y)}{\rho_0(y)} = \frac{p_0(y) + p_1(r)}{\rho_0(y) + \rho_1(r)} \tag{21}$$

Hence the density inside the tube differs from the field-free atmosphere by

$$\rho_1(r) = \frac{p_1(r)}{T_0(y)} \tag{22}$$

This initiates buoyant rise in the convection zone up to the convectively stable surface. The evolution of the flux tube is followed by solving eqns (10) to (14). The Coulomb resistivity η and the cowling resistivity η_c are calculated from the local density and temperature. The components of the current density $\mathbf{j}_\perp$ and $\mathbf{j}_\parallel$ are calculated at each timestep, and the resistive section of the induction equation (eqn 8) is sub-cycled within the ideal update to increase the efficiency of the code.

3. RESULTS

3.1. Emergence of flux

The initial phase of the tube's evolution involves buoyant rise to the surface. The evolution agrees with previous work of flux tubes in the convection zone, as in Magara and Longcope (2001) and Fan (2001). Once the tube meets the convectively stable layers of the atmosphere, there is a large expansion in the horizontal direction. A contact layer is formed with magnetic field holding up more plasma than if there were no field. Once enough flux has built up in this layer it becomes unstable to a Rayleigh-Taylor like instability called the magnetic buoyancy instability. This drives magnetic field through the chromosphere and into the corona (Archontis et al., 2004).

The effect of partial ionisation is investigated on the subsequent emergence of magnetic flux by comparing a fully ionised plasma model (FIP), where $\eta_c = 0$, to a partially ionised plasma model (PIP), where η_c is calculated from eqns (4) to (7).

The profile of η_c (Fig.1) represents a diffusive region of approximately 10 scale heights. As the magnetic buoyancy drives magnetic flux and plasma through the model chromosphere and into the corona, the presence of a diffusive layer in a partially ionised model atmosphere should affect the rate of emergence of this flux.

Flux emergence is estimated using the amount of unsigned vertical flux

$$\int |B_y| dx \tag{23}$$

where the integral is over the horizontal extent of the domain. Fig.3 show the total flux emerging at two different heights for the two models, as a function of time. The lower height is 500km, in the photosphere below the diffusive layer, and the upper height is 3000 km, in the corona above the diffusive layer. At the lower height the flux emerging for the FIP model and the PIP model are

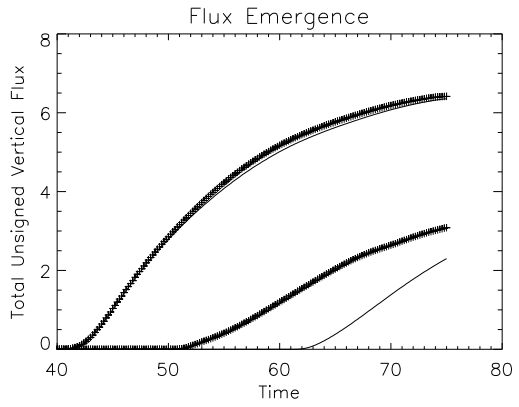

Figure 3. Total unsigned flux at constant heights as a function of time in the simulation. The two left plots are at heights 500km, and the two right plots are at 3000km above the surface. The solid lines are for the FIP model and the crosses are for the PIP model.

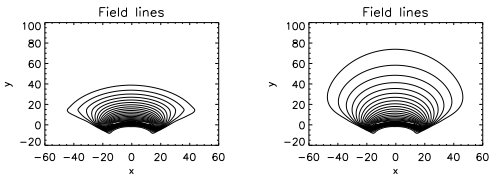

Figure 4. Fieldlines in x and y given by contours in A_z where $\mathbf{B} = \nabla \wedge \mathbf{A}$. The left panel is the FIP model, the right is the PIP model. Both plots use the same contour levels.

almost identical, as at this height $\eta_c = 0$ in both models. At 3000 km the flux emerging is greatly increased by the presence of the diffusive layer in the PIP model compared to the FIP model. As the magnetic field passes through this layer it is diffused on a timescale

$$t_d = \frac{L^2 \mu_0}{\eta_c} \tag{24}$$

where L is the vertical extent of the region. Inserting typical values gives $t_d \approx 5s$ which compares to the local transit time of flux across this region of $t_t \approx 500s$. Hence the magnetic field takes many diffusive timesteps to transit the partially ionised layer.

The resultant magnetic field structure is therefore different for the two models. Fig.4 shows 2D fieldlines in x and y for the two different models. The fieldlines are given by the contours in A_z where $\mathbf{B} = \nabla \wedge \mathbf{A}$. The resultant field is more diffuse in the PIP model, and the fieldlines extend higher into the atmosphere, which is as expected when an extra diffusive layer is added. The inclusion of the presence of neutrals in the simulation of emerging flux yields more rapid emergence and a greater amount of flux in the corona.

3.2. Cross-field and field-aligned currents

Observations of magnetic fields in the solar atmosphere suggest that the solar corona is predominantly force-free (Georgoulis and Labonte, 2004). The low β plasma of the solar corona is magnetically dominated, and the pressure and gravity terms in the momentum equation (eqn 12) are small in comparison to the Lorentz force. The equilibrium equation is given simply by

$$\mathbf{j} \wedge \mathbf{B} = 0. \tag{25}$$

This is equivalent to saying that the current is aligned with the magnetic field $\mathbf{j} \parallel \mathbf{B}$, or that there are no cross-field currents, $\mathbf{j}_\perp = 0$.

Beneath the surface the plasma β is much greater than unity, and therefore pressure forces dominate magnetic forces. The field in this region cannot be assumed to be force-free. If indeed, active regions are the product of emerging sub-surface field as evidence suggests (Zwann, 1977), then the force-free coronal field must be formed from non force-free fields. This raises an important question. How is the magnetic field of sub-surface flux tubes converted into force-free magnetic coronal field?

As stated in section 2.1, for a partially ionised plasma, the current is not diffused isotropically. Field-aligned currents ($\mathbf{j}_\parallel$) are diffused by the Coulomb resistivity η, and cross-field currents ($\mathbf{j}_\perp$) are diffused by η_c (eqn 8). However, it has been shown that η is effectively zero. This means that as the magnetic field emerges through the partially ionised region of the model atmosphere, the only component of the current to be diffused directly is the cross-field current.

This gives a mechanism for the formation of force-free current during flux emergence. As magnetic field is driven though the partially ionised layer by the magnetic buoyancy instability, cross-field currents are diffused by the ion-neutral interactions. While the field-aligned currents are not directly diffused. Hence if the value of η_c is large enough the field that emerges through the partially ionised region will have no cross-field currents and will therefore be force-free.

By comparing the amount of cross-field current emerging into the corona for the two models (FIP and PIP), the efficiency of this mechanism in forming force-free currents can be investigated. A measurement of the amount of cross-field current is obtained by performing the integral

$$J_\perp(y) = \int |\mathbf{j}_\perp(x, y)| \, dx, \tag{26}$$

over the horizontal extent of the domain. Fig.5 shows this as a function of height at t=75, for both the FIP and PIP models. The fully ionised plasma does not destroy cross-field currents and they are allowed to emerge into the corona with the magnetic field, giving a non force-free configuration. However, when the field emerges through a partially ionised plasma, nearly all of the cross-field

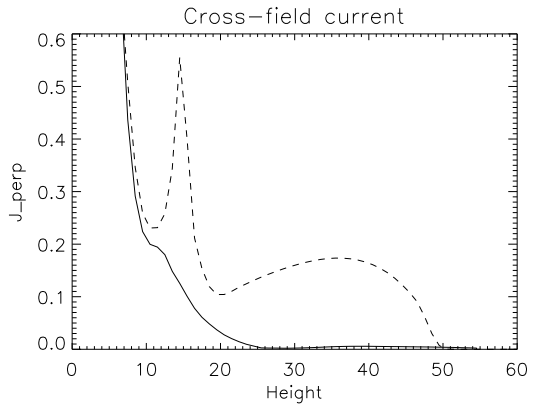

Figure 5. Total perpendicular current across the domain as a function of height for the FIP model (dashed line) and the PIP model (solid line). All values are given in normalised units.

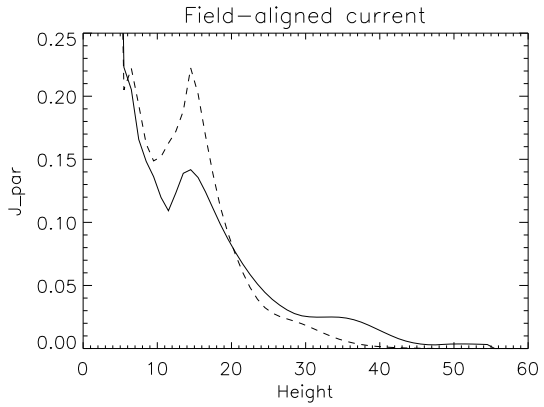

Figure 6. Total parallel current across the domain as a function of height for the FIP model (dashed line) and the PIP model (solid line). All values are given in normalised units.

current is destroyed, which corresponds to a force-free magnetic field.

Fig.6 shows the integral

$$J_{\parallel}(y) = \int \left|\mathbf{j}_{\parallel}(x,y)\right| dx, \qquad (27)$$

as a function of height at t=75 for both models. There is a small difference in $J_{\parallel}(y)$ for the two models. This is because the diffusion of parallel currents is coupled to the diffusion of perpendicular currents, which, as shown, is vastly different for the two models.

Evidently, the presence of a partially ionised region in the solar atmosphere has destroyed the cross-field current but allowed approximately the same amount of field-aligned current to emerge as in the case for a fully ionised plasma. Hence the field has been converted from a general configuration to one approaching a force-free state.

Calculations of the force-free nature of atmospheric magnetic field have been made based on observations using MDI (Georgoulis and Labonte (2004) and Metcalf et al. (1995)). Vector magnetograms have been extrapolated to reconstruct coronal field. Estimates of the height at which the field becomes force-free are typically 400-1000 km above the photosphere. A typical height for these simulations based on Fig.5 is much larger than this, around 2500 km. This discrepancy may lie in the 2D nature of the simulations, and further 3D work will be performed to better diagnose the height at which field becomes force-free. However, the emphasis of this work is on presenting a mechanism for the formation of force-free fields as standard models of flux emergence yield non-force-free fields in the corona. The emerging fields are force-free when a partially ionised model is used instead of a fully ionised one.

4. CONCLUSIONS

2.5D simulations of the emergence of magnetic flux through the partially ionised regions of the solar atmosphere have been performed. The relatively low temperatures in the chromosphere mean that the fully ionised approximation used in standard MHD is not valid everywhere in the simulation domain. The model was modified to include the effects of a partially ionised region. For a partially ionised plasma, the Coulomb resistivity η acts to diffuse currents parallel to the magnetic field, and the Cowling resistivity η_c diffuses currents perpendicular to the magnetic field.

We investigated the effect of partial ionisation on the emergence of magnetic flux using two models, fully ionised (FIP) and partially ionised (PIP) plasma models. The presence of neutrals lead to a large diffusive region, which only diffused currents perpendicular to the magnetic field. Hence not only was the magnetic field in the partially ionised model more diffuse with fieldlines extending further into the model corona, but no cross-field currents emerged with the field above 2500km, so the emerging field was force-free above this height. This compared to observational heights of below 1000km, the difference being due to the 2D nature of this work

To fully understand flux emergence it is necessary to work in 3D. The importance of shear forces and plasma draining in rising flux tubes has already been shown to be important for flux emergence (Manchester, 2001), as has the interaction with pre-existing coronal field Archontis et al. (2004). Future work will have to include all these effects, along with the methods applied in this work. Also the effect of joule heating, as given by $\eta_c {j_{\perp}}^2$, needs to be investigated relative to the other dynamics and thermal effects involved.

REFERENCES

Arber, T.D., Longbottom, A.W., Gerrard, C.L., Milne, A.M., 2001, JCP, 171, 151

Archontis, V., Moreno-Insertis, F., Galsgaard, K., Hood, A., O'shea, E., 2004, A&A, 2004, 426, 1047

Braginskii, S.I., Transport processes in a Plasma, in: Reviews of plasma physics, Vol1, Consultants Bureau, New York, 1965

Cowling, MagnetoHydroDynamics, Monographs on Astronomical Subjects, Adam Hilger, 1957

Fan, Y., 2001, ApJ, 554, L111

Georgoulis, M.K., LaBonte, B.J., 2004, 615, 1029

Gilman, P.A., Morrow, C.A., DeLuca, E.E., 1989, ApJ, 338, 528

Hughes, D.W., Proctor, M.R.E., 1988, Annu. Rev. Fluid. Mech., 20, 187

Khodahenko, M.L., Arber, T.D., Rucker, H.O., Hanslmeier, A., 2004, 422, 1073

Leake, J.E., Arber, T.D., Khodachenko, M.L., 2005, accepted in A&A

Magara, T., Longcope, D.W., 2001, ApJ, 559, 55

Manchester, W., 2001, ApJ, 547, 503

Metcalf, T.R., Jiao, L., McClymont, A.N., Canfield, R.C., 1995, 439, 474

Moreno-Insertis, F., Emonet, T., 1996, ApJ, 472, L53

Spitzer, L., 1962, Physics of fully ionised gases

Vernazza, J.E., Avrett, E.H., Loeser, R., 1981, ApJS, 45, 635

Zwann, C., 1977, SoPh, 60, 213